https://doi.org/10.5194/egusphere-2025-3035
Preprint. Discussion started: 7 July 2025

Simulating the effect of natural convection in a tundra snow cover

Mahdi Jafari[1] and Michael Lehning[1,2]

[1]CRYOS, School of Architecture, Civil and Environmental Engineering, EPFL, Lausanne, Switzerland.
[2]WSL Institute for Snow and Avalanche Research SLF, Davos, Switzerland.

Correspondence: Mahdi Jafari (mahdijafari.135@gmail.com)

Abstract. As a straightforward solution to improve the one-dimensional physics-based multi-layer snow model SNOWPACK, a C++ interface is implemented for a tight coupling between SNOWPACK and OpenFOAM with the aim to investigate natural convection in real snow covers. OpenFOAM simulates convection in two dimensions based on SNOWPACK snow profiles and feeds the convective vapor fluxes back to SNOWPACK. Among different snow covers, significant convection events that are well synchronized with cold events are numerically observed by the SNOWPACK-OpenFOAM coupler for a herb tundra permafrost at Bylot Island only if we neglect wind slab formation for surface layers. We find significant sublimation in downward flow regions and that convection generates a low-density path extending vertically almost through the whole snow column. The strong footprint of convection on snow density and temperature with significant lateral variations up to 90 kg m^{-3} and 5 K respectively makes a consistent representation in the SNOWPACK one-dimensional profile difficult. But the most prominent effect of convection on the snow density profile, namely a low density foot and high density top, corresponds qualitatively to observations. Further work is required to adapt physical parameterizations in conventional snow models to represent this effect and its interaction with snow settling and metamorphism.

1 Introduction

Water vapor transport is a significant dynamical process for shaping snow layers in snowpacks under strong temperature gradients, such as the Arctic and Subarctic ones (Trabant and Benson, 1972; Johnson and Bens, 1987; Alley et al., 1990; Sturm and Johnson, 1991; Domine et al., 2016, 2018). Strong temperature gradients (i.e low surface temperatures and comparably high base temperatures) in the snowpack produce strong gradients in water vapor density to develop a snow cover with a significant fraction of depth hoar layers (Derksen et al., 2009; Sturm and Benson, 1997; Taillandier et al., 2006; Domine et al., 2015). Measurements (Trabant and Benson, 1972; Alley et al., 1990; Sturm and Benson, 1997) suggest a continuous vapor flux from the soil into the basal snow layers, which are then losing vapor to upper layers. Sturm and Benson (1997) suggest that water vapor fluxes between snow layers result in mass change over finite distances and also change in layer density.

https://doi.org/10.5194/egusphere-2025-3035
Preprint. Discussion started: 7 July 2025

Water vapor diffusion alone is not sufficient for significant mass transfer at the base (Jafari et al., 2020; Domine et al., 2016) and convection is often considered as a dominant mechanism (Trabant and Benson, 1972; Johnson and Bens, 1987; Alley et al., 1990; Sturm and Johnson, 1991; Domine et al., 2016, 2018) for substantial mass transfer, which is an order of magnitude higher than calculated diffusive vapor fluxes (Trabant and Benson, 1972). However, convection of water vapor is not captured in convectional snow models leading to large errors in simulated snow properties. Domine et al. (2016) have underlined the difficulties of existing snowpack models to accurately simulate Subarctic snowpack layering, namely high density layers on top and lower density layers at the bottom. This is significant as such a profile enhances the insulating properties of the winter snow cover (Brun et al., 2009) and facilitates movement of animals over the hard surface snow (Vikhamar-Schuler et al., 2013). Recent field experiments further support that subnivean space created by low-conductivity basal snow is a critical thermal refuge for Arctic small mammals (Poirier et al., 2021). Moreover, snowpack stratigraphy directly affects species' winter habitat choice and predator avoidance (Reid et al., 2011; Duchesne et al., 2011), highlighting the ecological importance of accurately modeling snow density layering.

Jafari et al. (2020) studied the effects of diffusive water vapor transport on snow density for different snow covers by implementing vapor diffusion in SNOWPACK as a one-dimensional physics-based multi-layer snow model (Lehning et al., 1999; Bartelt and Lehning, 2002; Lehning et al., 2002b, a). However, the combined effects of convection and diffusion for water vapor transport have never been numerically investigated in combination with a full snow evolution model. In their study of a two-dimensional idealized snowpack, Jafari et al. (2022) employed a new physical model, named as *snowpackBuoyantPimpleFoam* (Jafari and Lehning, 2021), implemented in OpenFOAM 5.0 (www.openfoam.org), to analyze how convection of water vapor changes the snow structure laterally and vertically.

Significant differences remain between the observed and simulated snow density profiles, even when convection effects are included (as shown later in section 3). This indicates that the snow model itself requires adjustments for Arctic conditions, specifically through improvements in processes such as snow settling and wind compaction (Jafari, 2022). The convection model used in this paper is a direct numerical solution that shows an accuracy between 3% to 10% (Jafari et al., 2022). Therefore, to make meaningful comparisons between simulations and measurements, these processes need to be modeled with a similar level of accuracy, which currently cannot be achieved. It is important to explicitly state a key assumption underlying this study: the simulations conducted here adopt the default density stratification evolution of SNOWPACK, which are tailored to Alpine conditions. Arctic snowpacks, such as those found on Samoylov Island, are substantially influenced by wind compaction—a process for which no physically accurate, widely accepted model exists. The current parameterizations, including those proposed by Gouttevin et al. (2018), offer only a rough approximation. Including wind compaction in the simulation would likely result in a high-density surface layer that suppresses the formation of convection cells, rendering natural convection negligible. Therefore, we intentionally excluded wind compaction to isolate and analyze the effects of convection under conditions where it can dominate, namely persistent low surface temperatures and moderate snow depths (typically <1 m) that drive strong vertical temperature gradients. While this choice limits direct applicability to Arctic snow covers, it allows us to quantify the upper-bound

https://doi.org/10.5194/egusphere-2025-3035
Preprint. Discussion started: 7 July 2025

effects of vapor convection and to establish a framework for future modeling efforts that include wind compaction with similar physical rigor.

Since modeling convection in one-dimensional snow models is not possible, a direct solution to take into account the effects of convection for snow covers is to couple SNOWPACK with OpenFOAM. In this regard, the work presented in this paper brings us valuable insights: (1) the details in flow velocity, thermal, and phase change regimes can be analyzed for later parameterization of convection in one-dimensional snow models with no need to directly use OpenFOAM, (2) the effects of convection do not only substantially change the snow density vertically, but also induce a considerable and transient lateral heterogeneity in snow structure, (3) the induced lateral heterogeneity has a direct feedback on snow properties linked to the snow density such as the effective thermal conductivity and compaction, (4) the large difference between the temperature profiles in the upward and downward flow of a convection cell causes the temperature-dependent processes such as metamorphism and melting-refreezing to vary and actually also take place laterally in the snowpack.

2 Materials and Methods

As a straightforward solution to improve the one-dimensional physics-based multi-layer snow model, a C++ interface (dynamic library) is implemented for a tight coupling between SNOWPACK and OpenFOAM. Note that the detailed explanations, derivations, and model choices constituting the final set of equations for the convection simulation can be found in Jafari et al. (2022). As presented in Figure 1, the coupling procedure works as: (1) one SNOWPACK time step is solved taking into account all important processes such as settling, metamorphism, and melting-refreezing, (Lehning et al., 1999; Bartelt and Lehning, 2002; Lehning et al., 2002b, a) and (2) the snow height in OpenFOAM is dynamically synchronized with the new snow height from the SNOWPACK solution. Note that the dynamic mesh strategy used in the OpenFOAM solution is adding or removing layers only from the top. The minimum and maximum layer thicknesses are the thresholds given by the user to control the process for removing and adding a layer. Since the changes in both ice and water contents are updated from the SNOWPACK solution, there is no need to change the size of internal elements in the OpenFOAM. (3) the snow density change will be interpolated from the SNOWPACK solution to the OpenFOAM domain uniformly in the lateral direction as will be explained later in item (i), (4) after the information exchange between the two solvers, the two-dimensional natural convection is solved by OpenFOAM to update the snow density change due to vapor transport. (5) the horizontal average of the snow density change rate in OpenFOAM is interpolated for each element of SNOWPACK. The assumptions and limitations considered for SNOWPACK-OpenFOAM coupling are explained as follows:

(i) For new snow elements in the OpenFOAM domain, all the snow parameters are directly interpolated from the SNOWPACK output with uniform distribution in the lateral direction. For previously formed snow elements, the snow density change due to snow compaction (settling), water transport, and melting-refreezing process from the SNOWPACK solution is considered as: (1) In the OpenFOAM domain, the cumulative changes in both ice and water volumetric contents due to vapor transport are stored as $\Delta\theta_{i,cum_{vap},OF}$ and $\Delta\theta_{w,cum_{vap},OF}$ respectively, (2) the absolute changes in both ice

https://doi.org/10.5194/egusphere-2025-3035
Preprint. Discussion started: 7 July 2025

and water volumetric contents due to vapor transport in the SNOWPACK solution (already given from the OpenFOAM solution) are stored as $\Delta\theta_{i,vap,SN}$ and $\Delta\theta_{w,vap,SN}$ respectively, (3) then, these absolute and cumulative changes due to vapor transport are subtracted from the new ice and water content calculated in SNOWPACK as $\theta_{i,SN}$ and $\theta_{w,SN}$ respectively, (4) finally, after the SNOWPACK solution, the new ice and water content in the OpenFOAM domain may be calculated as $\theta_{i,OF} = \theta_{i,SN} - \Delta\theta_{i,vap,SN} + \Delta\theta_{i,cum_{vap},OF}$ and $\theta_{w,OF} = \theta_{w,SN} - \Delta\theta_{w,vap,SN} + \Delta\theta_{w,cum_{vap},OF}$ repressively. Note further that for any required quantities for the information exchange between the SNOWPACK and OpenFOAM domains, the interpolation process is done by comparing the height of an element in OpenFOAM with element heights in SNOWPACK. This implies that the interpolation from the SNOWPACK solution is done uniformly in the lateral direction into the OpenFOAM domain. Adding or removing layers is governed by criterion of minimum and maximum layer thicknesses, chosen as 0.005 m and 0.01 m, respectively. These values are consistent with a chosen value of 0.0075 mm for the height of a new element in SNOWPACK to have almost the same number of elements in both SNOWPACK and OpenFOAM, which is important to preserve layer properties in the profiles when interpolating between SNOWPACK and OpenFOAM.

(ii) The only feedback from OpenFOAM to SNOWPACK is laterally-averaged snow density change rate due to water vapor transport. However, because of convection effects, laterally-averaged temperature profiles would be different from the SNOWPACK solution. In the future, (1) the averaged temperature profiles from the OpenFOAM solution can be used as an initial temperature profile for the next time step of SNOWPACK, and (2) the interpolated density change rate due to vapor transport from the OpenFOAM solution will be used for the metamorphism calculation in SNOWPACK. Note that thermal boundary conditions in OpenFOAM for the top and bottom boundaries will be set from the SNOWPACK solution. It is worth mentioning that it would theoretically be possible to use several parallel SNOWPACK solutions in the lateral direction in the OpenFOAM domain. Because of lateral heterogeneity in snow density (as discussed later in section 3), the snow compaction is different and this would result in different snow heights for each SNOWPACK solution. This makes a discontinuity on the top boundary and prevents the use of the same dynamic mesh strategy in OpenFOAM used in this paper (only one SNOWPACK solution for the whole OpenFOAM domain). To address this problem for the future work, from the numerical modeling perspective in OpenFOAM it is possible for each SNOWPACK domain to have its own mesh which is disconnected from the neighbouring meshes (the neighbouring SNOWPACK domains). However, careful attention needs to be made (1) to meaningfully set up the thermal and flow boundary conditions at the discontinuity patches on top, and (2) for the information exchange between neighbouring meshes (each SNOWPACK solution) in the OpenFOAM domain. Note that in the SNOWPACK-OpenFOAM coupling, the soil part is only considered in SNOWPACK as convection is unlikely to occur in the soil. However, when using several parallel SNOWPACK solutions in the lateral direction of the OpenFOAM domain, it will be possible to represent the lateral thermal variations at the bottom of snowpack for the OpenFOAM solution as suggested by (Jafari and Lehning, 2023).

(iii) In case of melting-refreezing and water transport, (1) the water transport is only modelled by SNOWPACK, (2) the phase change calculation for melting-refreezing process in SNOWPACK is treated explicitly and therefore the temperature

https://doi.org/10.5194/egusphere-2025-3035
Preprint. Discussion started: 7 July 2025

is forced to be the melting temperature in SNOWPACK, (3) however, in OpenFOAM, thermal equilibrium is assumed between the ice and water while the local thermal non-equilibrium model is still considered between the ice-water mixture and the gas phase. Similarly, for melting-refreezing process in OpenFOAM, melting temperature is assigned for the ice-water mixture. Note that in case the short wave radiation is large enough to increase the ice temperature in OpenFOAM above melting, we limit it by the melting temperature (as it is explicitly done in SNOWPACK for melting-refreezing process) and therefore we do not directly use the heat source/sink term from melting-refreezing in OpenFOAM. The heat transfer equations for the ice-water mixture and the gas phase are similar to those presented in Jafari et al. (2022) except for the changes due to presence of water and the heat source/sink term from shortwave radiation absorption. The energy equations with above mentioned changes compared to ones in Jafari et al. (2022) in terms of temperature for the gas phase and ice-water mixture are presented as:

$$\frac{\partial}{\partial t}(\epsilon_g \langle\rho_g\rangle^g c_{pg} \langle T_g\rangle^g) + \nabla\cdot(\langle\rho_g\rangle^g c_{pg} \langle T_g\rangle^g \langle \boldsymbol{U}_g\rangle) = \nabla\cdot(\epsilon_g k_{\text{eff},g} \nabla \langle T_g\rangle^g)$$
$$+ \epsilon_g \frac{\partial}{\partial t}\langle P_g\rangle^g + \langle \boldsymbol{U}_g\rangle \cdot \nabla \langle P_g\rangle^g - \nabla\cdot[\langle T_g\rangle^g (c_{pv} - c_{pa}) \langle J_v\rangle]$$
$$+ h_c a_s \left[(\langle T_g\rangle^g (w_g - 1) - \langle T_i\rangle^i w_i)\right] + (\dot{m_{iv}} + \dot{m_{wv}}) c_{pv} \langle T_g\rangle^g \quad (1)$$

$$\frac{\partial}{\partial t}(\rho_i c_{pi} \epsilon_i \langle T_i\rangle^i + \rho_w c_{pw} \epsilon_w \langle T_i\rangle^i) = \nabla\cdot(\epsilon_i k_{\text{eff},i} \nabla \langle T_i\rangle^i + \epsilon_w k_{\text{eff},w} \nabla \langle T_i\rangle^i)$$
$$- h_c a_s \left[(\langle T_g\rangle^g (w_g - 1) - \langle T_i\rangle^i w_i)\right]$$
$$- \dot{m_{iv}} c_{pv} (\langle T_g\rangle^g w_g + \langle T_i\rangle^i w_i) - \dot{m_{iv}} (c_{pi} - c_{pv}) T_{\text{ref}} - \dot{m_{iv}} L_{iv}$$
$$- \dot{m_{wv}} c_{pv} (\langle T_g\rangle^g w_g + \langle T_i\rangle^i w_i) - \dot{m_{wv}} (c_{pw} - c_{pv}) T_{\text{ref}} - \dot{m_{wv}} L_{wv}$$
$$+ Q_{swr} \quad (2)$$

In the above equations, respectively, ϵ_i, ϵ_w, ϵ_g are the volume fractions for ice, water, and gas phase, $\dot{m_{wv}}$ and $\dot{m_{iv}}$ are the rates of phase change from water to vapor and from ice to vapor, ρ_i, ρ_w, ρ_g are the densities for ice, water, and gas phase, c_{pi}, c_{pw}, and c_{pg} are the specific heat capacities for ice, water, and gas phase, $\langle T_i\rangle^i$ is the temperature of water-ice mixture and it is the ice temperature if the water is absent, $k_{\text{eff},i}$, $k_{\text{eff},w}$, and $k_{\text{eff},g}$ are the effective thermal conductivities of ice, water, and the gas phase in snow, $\langle \boldsymbol{U}_g\rangle$ is the bulk gas-phase velocity vector, $\langle P_g\rangle^g$ is the gas pressure, h_c is the heat transfer coefficient, a_s is the specific surface area, $T_{\text{ref}} = 273.15$ K is the reference temperature, and finally Q_{swr} is the heat source due to shortwave radiation absorption. Many of the parameters defined here are the same as presented in Jafari et al. (2022). Note that (1) the thermal conductivities are calculated by a parametrization presented in Lehning et al. (2002b) and used in SNOWPACK and they are indeed extracted from the definition of the effective thermal conductivity of

https://doi.org/10.5194/egusphere-2025-3035
Preprint. Discussion started: 7 July 2025

snow as $k_{\text{eff},s} = \epsilon_i k_{\text{eff},i} + \epsilon_w k_{\text{eff},w} + \epsilon_g k_{\text{eff},g}$ (Calonne et al., 2012; Hansen and Foslien, 2015), (2) the calculation of the mass transfer coefficient between ice and vapor, introduced as h_m in Jafari et al. (2022), is also assumed the same between water and vapor, and (3) the specific surface area a_s is calculated as explained in Jafari et al. (2020) when both water and ice are present.

(iv) For the calculation of all parameters dependent on the grain diameter such as specific surface area, the pore Reynolds number and snow permeability, we use the "classical" grain size not the optical grain diameter. SNOWPACK provides both the classical (heuristic) grain size as r_g and optical grain size as r_{osg} which is directly linked to the specific surface area (Calonne et al., 2012) but only a parameterized quantity in SNOWPACK. Based on the simulations in this paper, the values for r_{osg} are often smaller in particular at the bottom of snowpack by a factor of two. For the calculation of permeability and other flow properties, classical grain size is considered more pertinent than optical grain size.

(v) Within one time step of SNOWPACK (15 min is chosen in this study), OpenFOAM integrates over several smaller adjustable time steps based on the maximum Courant number of 5. Note that it is possible to use the PIMPLE algorithm for higher values of the maximum Courant number in OpenFOAM as employed in Jafari et al. (2022), but as the thermal boundary condition is changing through the SNOWPACK solution and therefore there is a transient thermal process, it is faster to use the smaller maximum Courant number of 5 (numerically stable) with the PISO algorithm (Moukalled et al., 2016). Note that within a 15 min time interval for coupling, for the first few minutes in OpenFOAM there are transient changes for the thermal regime and the flow velocity and after that it will be often (not always) a near steady-state process till the end of 15 min time interval. Therefore, to avoid computational cost, it is possible to freeze the thermal and flow calculation in OpenFOAM for the steady-state part of a 15 min time interval and only update the snow density change due to vapor transport. We call this strategy a "flow-freezing" time integration and we use the threshold of 60 s after which the thermal and flow calculation in OpenFOAM is stopped till the end of 15 min time interval. We performed simulations with full transient time integration and compared it to "flow freezing" for only the first two months of a winter season in Bylot herb tundra. We found that (1) it takes 21 hours (with four MPI processors) of computer runtime while it takes only 5 hours with "flow-freezing" and (2) the averaged cumulative density changes have shown acceptably small differences. It is further important to mention that the calculated snow density change rate due to vapor transport from OpenFOAM to SNOWPACK is chosen at the end of 15 min time interval and not averaged over 15 min, based on the same assumption that a quasi-steady state situation is attained. Time averaged snow density change rates over 15 min time interval in OpenFOAM would be a better choice if transient effects within the 15 minutes time step are important.

(vi) Thermal dispersion and hydrodynamic dispersion (for mass transfer) are not considered in this study. Thermal and hydrodynamic dispersion coefficients are often considered as an additional tensorial term added to the effective thermal conductivity and vapor diffusivity, respectively. These coefficients are important for strong advection and convection, i.e. when the pore Péclet number $Pe_p = ScRe_p > 1$ with Sc the Schmidt number and Re_p the pore Reynolds number (Bear, 1961, 1988; Calonne et al., 2015). For convection in idealized snowpacks as reported by Jafari et al. (2022), the pore Reynolds number and consequently Péclet number are smaller than 1. However, based on the results in this paper

https://doi.org/10.5194/egusphere-2025-3035
Preprint. Discussion started: 7 July 2025

for convection in real snowpacks (Bylot herb tundra), for the first few centimeters from the bottom of the snowpack in downward flow and only when convection forms low density patches there, the pore Péclet number can reach values up to 10. Note that as mentioned in item (iv), these results are based on the classical grain size which often induces larger snow permeability and flow velocity. Using the optical grain size (lower snow permeability and flow velocity), the pore Péclet number would remain smaller up to 2.8. For the gas flow in the porous medium with randomly packed spheres based on Delgado (2007), the ratio of hydrodynamic dispersivity to diffusivity is on the order of the Péclet number for $1 < Pe_p < 10$. Thus, effects of dispersion could be locally important and should further be explored. Nield and Bejan (2017); Kvernvold and Tyvand (1980) discuss that thermal dispersion does not affect the critical Rayleigh number which is based of effective molecular diffusivity but it can influence the flow structure in a convection cell (Nield and Bejan, 2017; Wen et al., 2018; Fahs et al., 2020).

In summary, for the OpenFOAM solution as presented in detail in Jafari et al. (2022), an Eulerian–Eulerian two-phase approach is used to solve mass conservation equations for the gas mixture (humid air), water vapor component, and mixture of ice and water phases, the momentum equation for the gas mixture, and finally the temperature-based energy equations for the gas, and mixture of ice and water phases. Therefore, the numerical output from the OpenFOAM solver provides solutions for water vapor and air densities, snow porosity and density, the gas flow velocity, the diffusive water vapor flux, the phase change rate between the mixture of ice and water phases and vapor, and finally the temperature for the gas and mixture of ice and water phases.

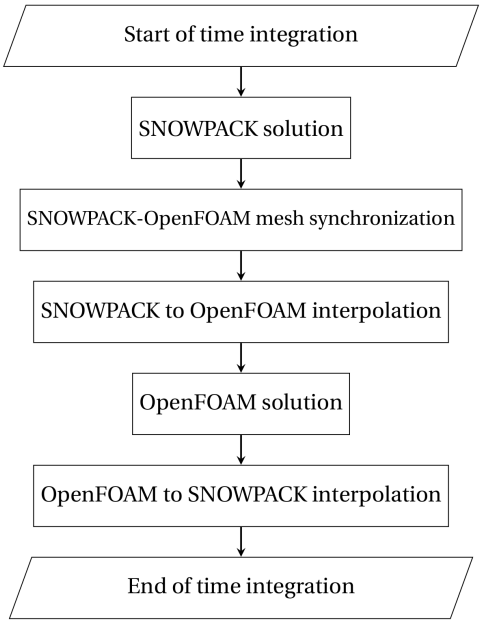

Figure 1. The coupling procedure between SNOWPACK and OpenFOAM.

https://doi.org/10.5194/egusphere-2025-3035
Preprint. Discussion started: 7 July 2025

3 Results and Discussion

For thick snow covers (e.g. Alpine and sub-arctic), no convection of water vapor has been observed in our numerical analysis because of both insufficient temperature gradients and high snow density. However, for a herb tundra permafrost site, situated at Bylot Island, Canadian high Arctic, conditions to trigger convection are at least partially fulfilled. Forcing data from observations for snow depth and surface temperature (Domine et al., 2021) are used to drive the SNOWPACK model. The following results presented for Bylot herb tundra are based on assumptions and limitations explained in section 2. As mentioned in item (iv) of section 2, the normal grain size from SNOWPACK is used, which is often larger than the optical grain size. Obviously, using the optical grain size would induce lower flow velocities and the results will be quantitatively different. Also, we used the measured snow heights and surface temperatures to drive the SNOWPACK model. Using the precipitation and heat fluxes to drive SNOWPACK often leads to much colder temperature regimes.

Here, we analyse the effects of convective water vapor transport at Bylot over tundra permafrost for three winter seasons. The time series for the temperature profiles due to only diffusive vapor transport from SNOWPACK simulations are shown in figure 2. As can be seen in this figure, there are several persistent cold events, some of which have been active for a few months. For instance, during the winter season 2017-2018, there were three main cold events, the second of which began on December 15 and lasted for three months and a half with almost no change in the snow height.

https://doi.org/10.5194/egusphere-2025-3035
Preprint. Discussion started: 7 July 2025

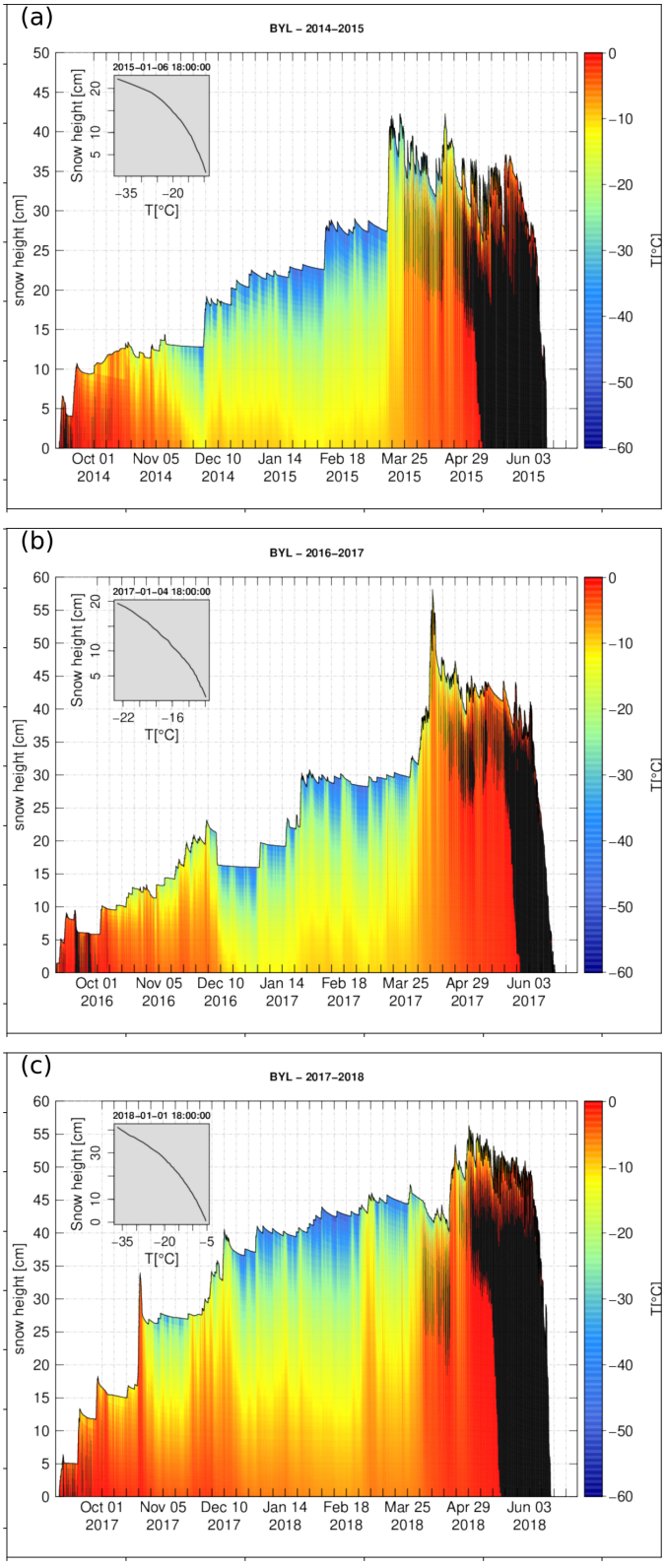

Figure 2. The time series of snow temperature from SNOWPACK simulation with only diffusion in Bylot herb tundra for (a) winter season 2014-2015, (b) winter season 2016-2017, and (c) winter season 2017-2018. The insets show the vertical profiles on early January for all three years. Black color refers to zero values.

https://doi.org/10.5194/egusphere-2025-3035
Preprint. Discussion started: 7 July 2025

SNOWPACK simulations with only diffusion are compared to those with convection from SNOWPACK-OpenFOAM simulations, as shown in figure 3 and figure 4 for cumulative density change and in figure 5 and figure 6 for density change rate due to water vapor transport. At Bylot, a large enough temperature difference and low enough snow density fulfill the conditions for significant and persistent convection events that are well synchronized with cold events. For example, during these cold events, SNOWPACK-OpenFOAM simulations show higher values of snow density change rate compared to SNOWPACK simulations (comparing figure 5a with figure 5b for winter season 2016-2017, and figure 6a with figure 6b for winter season 2017-2018). This also shows a meaningful difference in snow density change when compared to diffusion from SNOWPACK simulations, particularly for the snow density increase in the deposition zone. For example, the cumulative snow density change is increased by 35 kg m^{-3} in the winter season 2017-2018 whereas the increase by diffusion from SNOWPACK simulations is small and around 5 kg m^{-3} (comparing figure 4a to figure 4b). This would be even larger and around 55 kg m^{-3} for local cumulative density change as is shown in figure 9f for two-dimensional profiles. Note that as explained by Jafari et al. (2020), cumulative snow density is introduced as the summation of snow density change due to the sublimation and deposition of water vapor for each element over all time steps.

More cumulative density change with a different profile is also observed from SNOWPACK-OpenFOAM results compared to diffusion alone from SNOWPACK simulations. This can be seen by comparing the subplots of figure 3 for winter season 2016-2017 and figure 4 for winter season 2017-2018. Moreover, an effective depth of about 10-20 cm is observed for decreased snow density by convective vapor transport (figure 7a and e) while for diffusive vapor transport, the reduced snow density is mainly observed for a thin layer close to the ground (figure 7a, c and e). Similarly, the density profiles observed before the melt season from SNOWPACK-OpenFOAM simulations, have an obvious shift and decrease compared to diffusion-only results (figure 7b, d and f). A decrease in density is not limited only to layers close to the ground and it can be seen almost through the whole lower snow column, amounting up to 60 kg m^{-3} (figure 7a, d, and f).

https://doi.org/10.5194/egusphere-2025-3035
Preprint. Discussion started: 7 July 2025

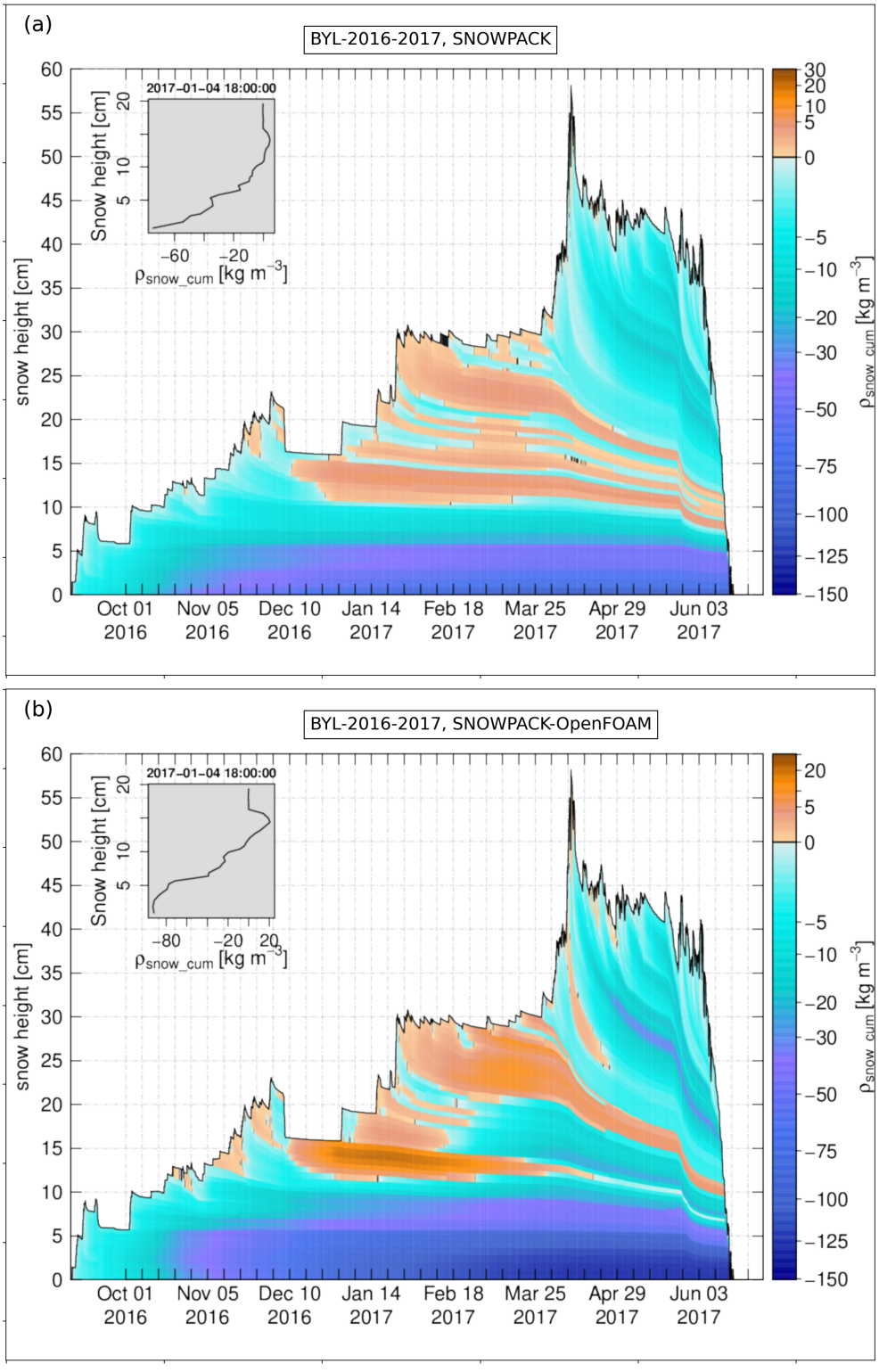

Figure 3. The time series of cumulative density change for winter 2016-2017 in Bylot herb tundra, (a) SNOWPACK simulation with diffusion and (b) SNOWPACK-OpenFOAM simulation with convection. The insets in (a) and (b) show the vertical profiles on 4 January 2017 18:00:00. Black color refers to zero values.

https://doi.org/10.5194/egusphere-2025-3035
Preprint. Discussion started: 7 July 2025

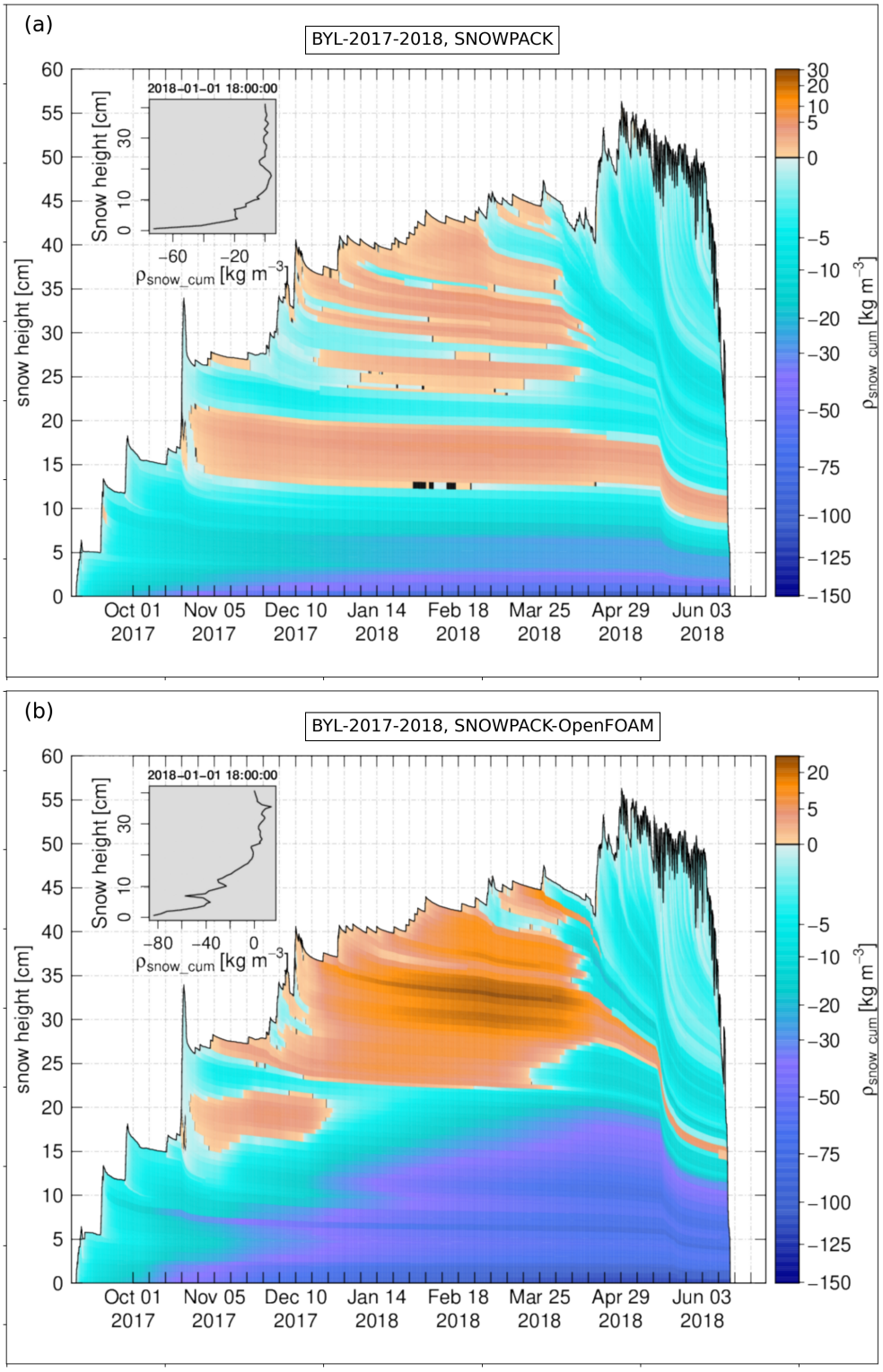

Figure 4. The time series of cumulative density change for winter 2017-2018 in Bylot herb tundra, (a) SNOWPACK simulation with diffusion and (b) SNOWPACK-OpenFOAM simulation with convection. The insets in (a) and (b) show the vertical profiles on 1 January 2018 18:00:00. Black color refers to zero values.

https://doi.org/10.5194/egusphere-2025-3035
Preprint. Discussion started: 7 July 2025

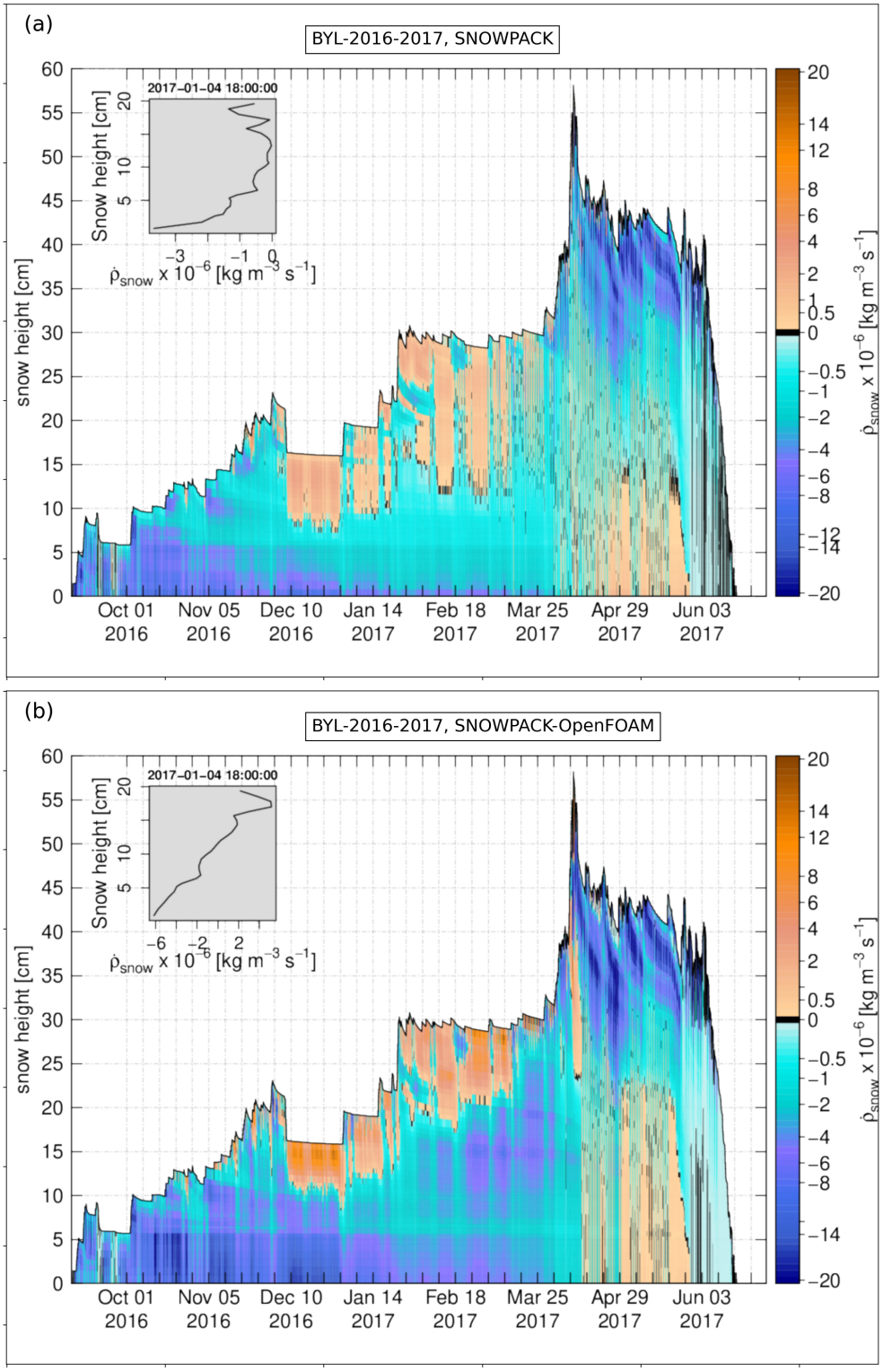

Figure 5. The time series of snow density change rate due to vapor transport for winter 2016-2017 in Bylot herb tundra, (a) SNOWPACK simulation with diffusion and (b) SNOWPACK-OpenFOAM simulation with convection. The insets in (a) and (b) show the vertical profiles on 4 January 2017 18:00:00. Black color refers to zero values.

https://doi.org/10.5194/egusphere-2025-3035
Preprint. Discussion started: 7 July 2025

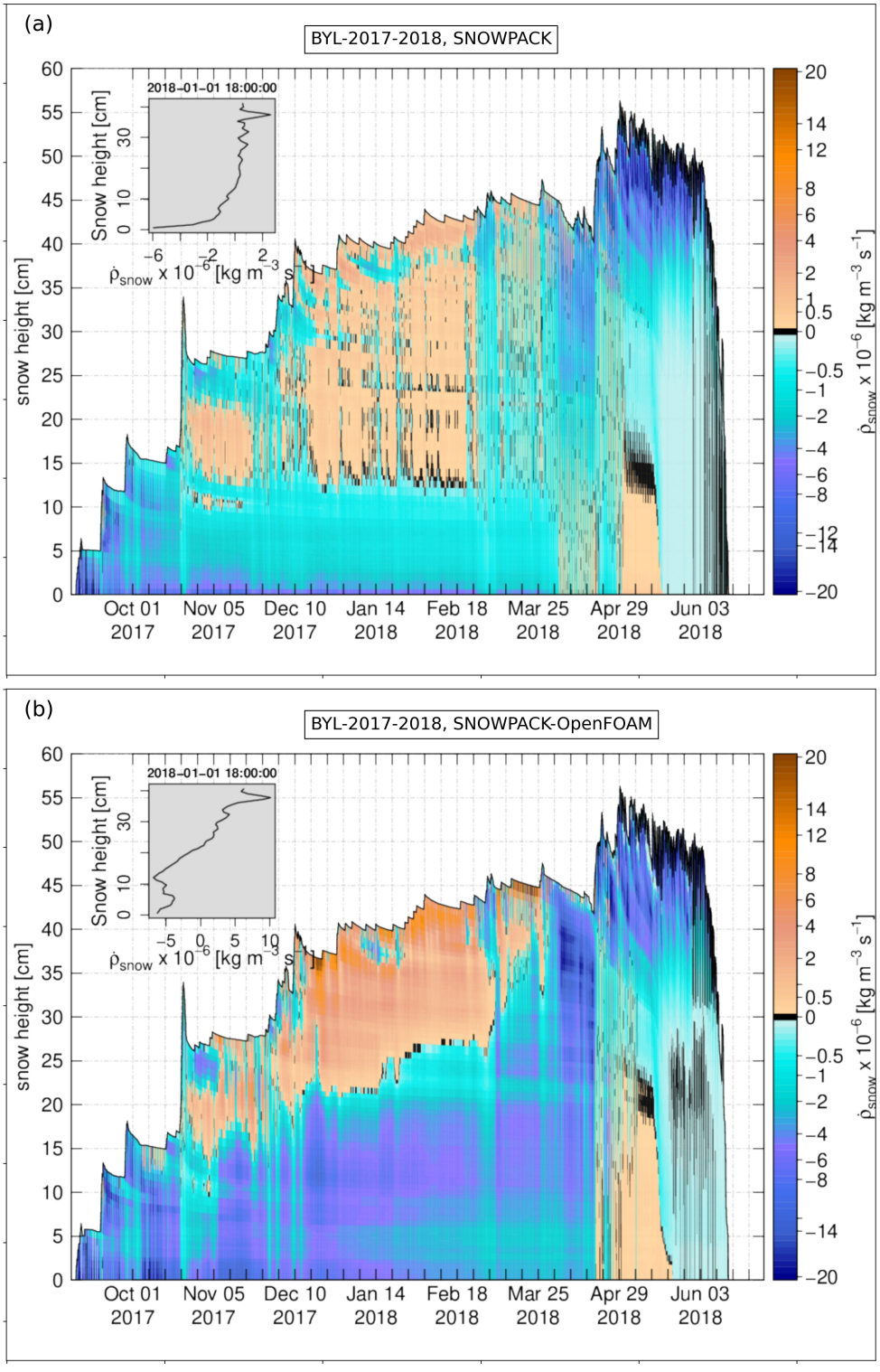

Figure 6. The time series of snow density change rate due to vapor transport for winter 2017-2018 in Bylot herb tundra, (a) SNOWPACK simulation with diffusion and (b) SNOWPACK-OpenFOAM simulation with convection. The insets in (a) and (b) show the vertical profiles on 1 January 2018 18:00:00. Black color refers to zero values.

https://doi.org/10.5194/egusphere-2025-3035
Preprint. Discussion started: 7 July 2025

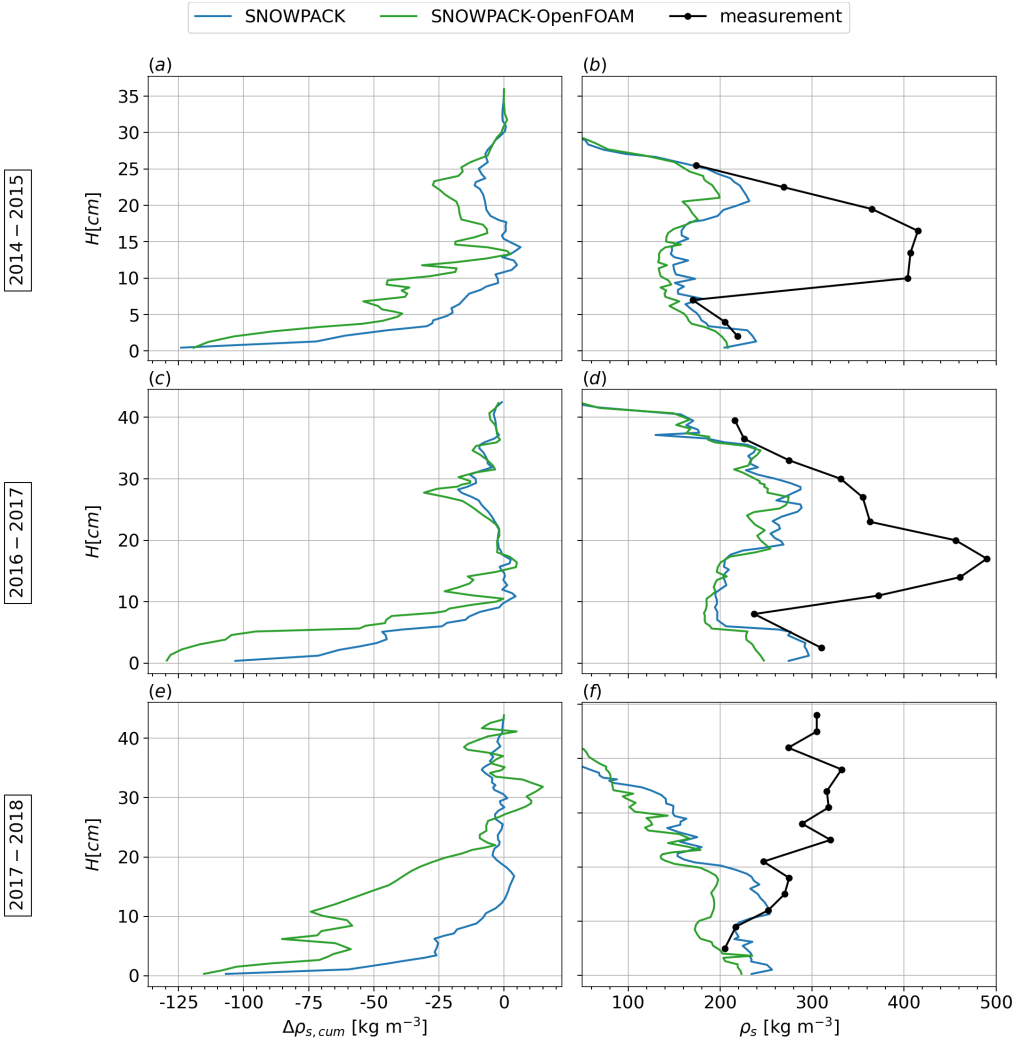

Figure 7. Comparison between diffusion from SNOWPACK simulation and convection from SNOWPACK-OpenFOAM simulation for cumulative snow density change and snow density profiles on 12 April 2015 12:00:00 for winter season 2014-2015, 13 May 2017 12:00:00 for winter season 2016-2017, and 14 April 2018 12:00:00 for winter season 2017-2018.

As an example, we focus on the winter season 2017-2018 to explore the effects of convection on the thermal and phase change regimes and how it laterally and vertically changes the snow density and temperature. To do this, the two-dimensional profiles for snow density are shown in figure 8 at the end of second cold event on March 11. As can be seen, the convection cells have the same lateral pattern for shaping the snow density profile. Time snapshots to show the evolution in snow density due to convective water vapor transport for the beginning (December 14), middle (January 26), and end (March 11) of the second cold event are shown in figure 9. For the first snapshot, we do not see a large footprint of convection in the snow density (figure 9a) but we can already observe the initial changes in the cumulative snow density (figure 9d). As indicated in figure 9 for phase

https://doi.org/10.5194/egusphere-2025-3035
Preprint. Discussion started: 7 July 2025

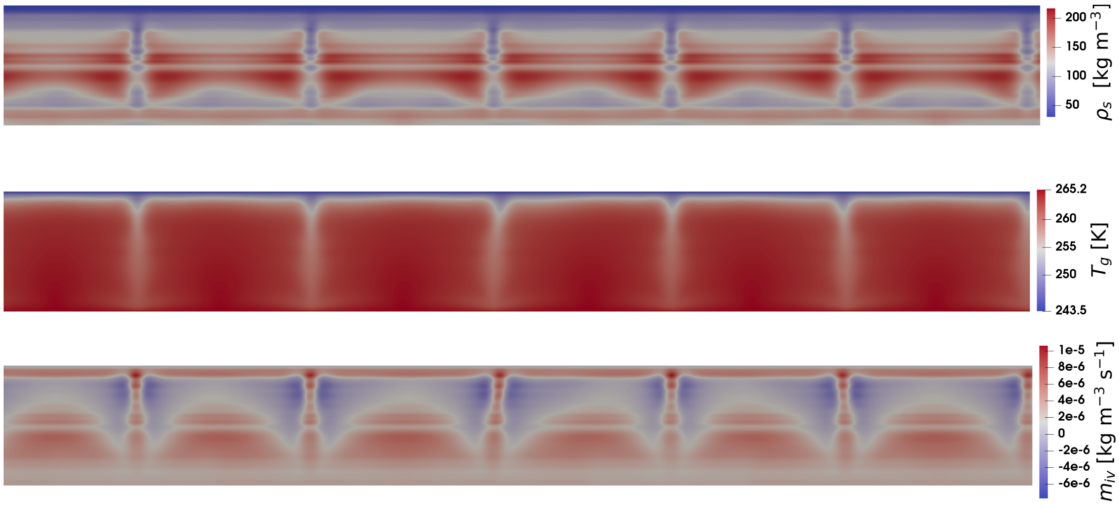

Figure 8. Simulated two-dimensional plots from SNOWPACK-OpenFOAM coupling on 11 March 2018 12:00:00 for (a) snow density, (b) the gas phase temperature, and (c) the phase change rate from ice to vapor.

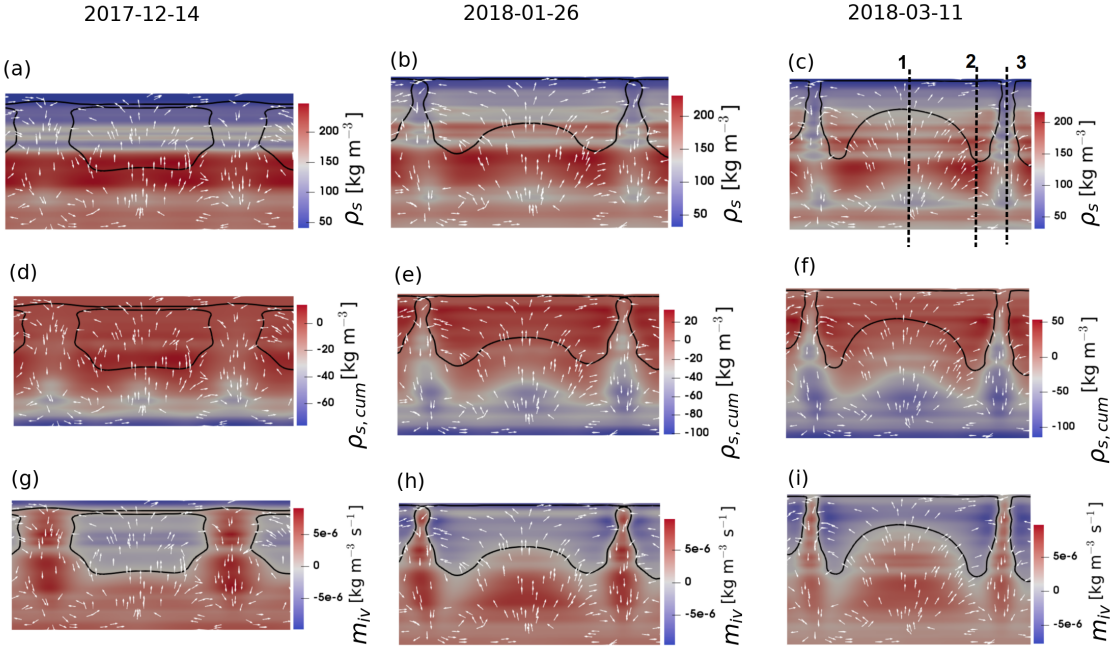

Figure 9. Evolution of snow density, cumulative snow density change, and phase change rate from ice to vapor for different dates as December 14, January 26, and March 11 in the winter season 2017-2018. The white arrows show the flow direction and are not scaled with the velocity magnitude.

https://doi.org/10.5194/egusphere-2025-3035
Preprint. Discussion started: 7 July 2025

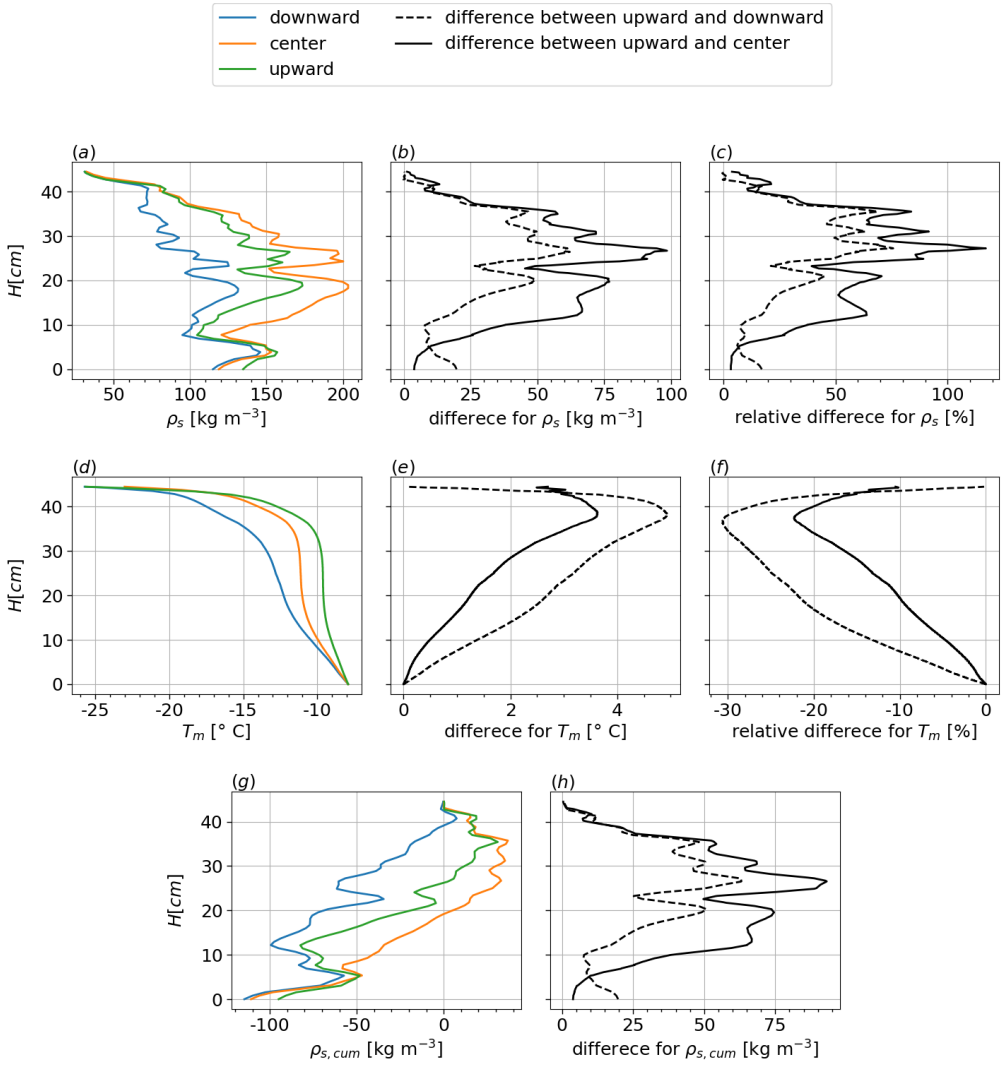

Figure 10. Lateral variations in a convection cell for the snow density, temperature, and cumulative snow density change due to water vapor transport. These profiles are plotted over three vertical lines as drawn in figure 9c on March 11 in winter seasons 2017-2018.

https://doi.org/10.5194/egusphere-2025-3035
Preprint. Discussion started: 7 July 2025

change from ice to vapor, for all three snapshots, we can see that sublimation is significant for the whole downward flow and not only for the layer close to the ground. This is different from what we observed for the effective sublimation zone in idealized snowpacks discussed in Jafari et al. (2022). For the second time snapshot (middle of the second cold event on December 14), the sublimation can already create a vertical low density path through a significant depth of the snow to consequently have increased flow velocity in the whole downward flow. This process continues till the end of the second cold event such that the convection cells gets stronger and more stable over time and stay at their initial location. Here, we do not see the lateral displacement of the convection cells, which is again different from what we indicated for idealized snowpacks in Jafari et al. (2022).

One more different observation for convection in SNOWPACK generated snow covers from the one in idealized snowpacks is that the deposition zone often expected to be on top in the upward flow is increasingly distorted toward the region of downward flow as time progresses. Although the convection cells do not migrate laterally, the flow-blocking process in upward flow due to deposition still distorts the deposition zone toward the region on top between downward and upward flows (figure 9c).

Furthermore, as can also be seen from figure 10, significant lateral variations within a convection cell are present on OpenFOAM-SNOWPACK coupling for snow density, cumulative snow density change, and snow temperature. In figure 10, profiles are plotted over three different vertical lines (as drawn in figure 9c) i.e. line 1 for upward flow, line 2 between upward and downward flows, and finally line 3 for downward flow. For example, lateral differences up to 90 kg m^{-3} (115%) are observed for snow density (figure 10b and c) and up to 5 K (30%) for snow temperature (figure 10f and g) at the end (March 10) of the second cold event in the winter season 2017-2018.

The sensitivity analysis on the horizontal domain length shows that the smaller domain length has a small effect on snow density (figure 11). This is important as it helps considerably to reduce computational time. As explained in item (v) of section 2, to reduce computational time, the "flow freezing" strategy is used. Figure 12 shows that the difference from "full integration" case is small for snow density. We point out, however, that the snow density change rate and flow velocity are similar only for moderate convection events and they are quite different for the strong convection events observed at the end of the second month in the winter season. These values are smaller for "flow-freezing" again in particular at the bottom of the snowpack (smaller by a factor of two), where strong grain growth leads to stronger convection. This implies that we may underestimate the effects of convection when using "flow-freezing". Further sensitivity studies are needed to explore this effect together with the grain size representation.

4 Conclusions, Limitations and Outlook

In this paper, convective vapor transport in herb tundra snow covers and its effects on snowpack structure have been investigated numerically, assuming no wind compaction occurs to increase snow density at the surface. This assumption was made to isolate the influence of natural convection, given that no physics-based model currently exists for wind compaction with a level of accuracy comparable to the convection model employed. Including wind compaction, for example via available parameterizations, would result in a high-density surface layer that suppresses convection almost entirely. As such, the results presented should be interpreted as representing the upper limit of convective effects, particularly under conditions characterized

https://doi.org/10.5194/egusphere-2025-3035
Preprint. Discussion started: 7 July 2025

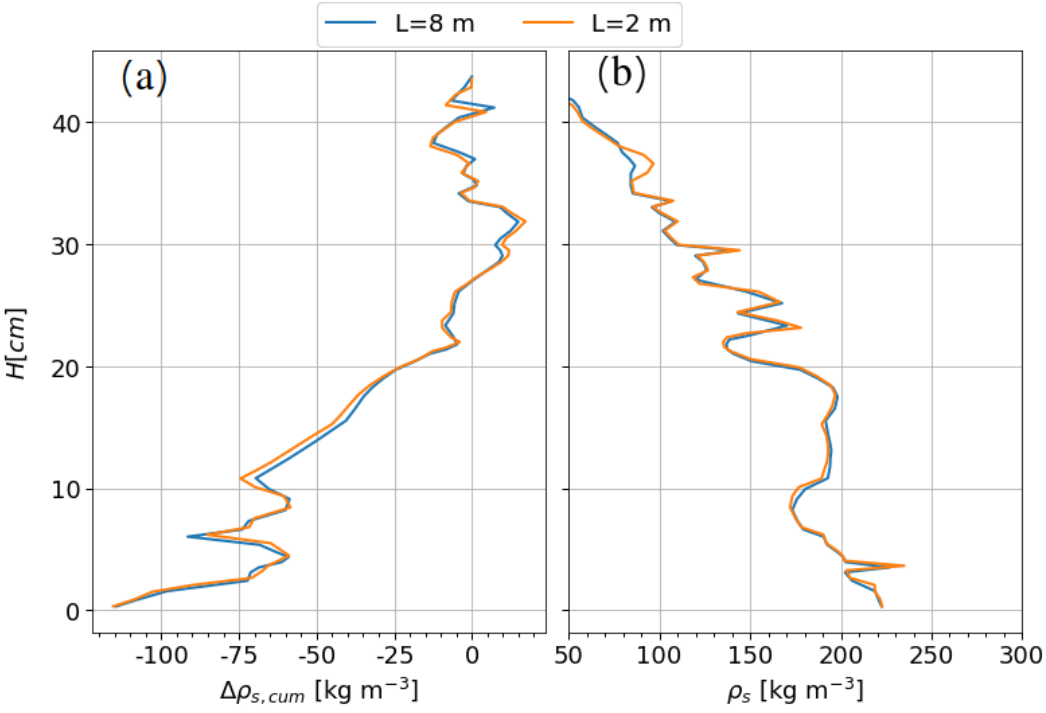

Figure 11. The sensitivity analysis on the horizontal domain length for winter 2017-2018 on 14 April 2018 12:00:00 in Bylot herb tundra, (a) cumulative density change and (b) snow density. Here, L is the horizontal domain length.

by persistent cold surface temperatures and moderate snow depths (typically less than 1 m), where strong temperature gradients promote natural convection. To that end, a C++ interface has been implemented for a tight coupling between SNOWPACK and OpenFOAM.

Looking at time series of temperature profiles, it is found that strong snow density change rates due to sustained convection are strongly linked to persistent cold events observed for Bylot tundra. Compared to diffusion results, a larger increase in cumulative snow density change up to 55 kg m^{-3} is observed close to the snow surface. Furthermore, it is shown that a significant decrease in snow density due to convective vapor transport (up to 60 kg m^{-3}) is not limited only to a small layer at the base but it has an effective depth of about 10-20 cm, which corresponds better to observations. However, even under the unrealistic assumption of low density surface snow, the density changes both negative at the foot and positive at the surface are insufficient to fully explain observed profiles.

Investigating lateral and vertical effects of convection on the thermal and phase change regimes for Bylot, it is found that convection cells qualitatively have the same lateral footprint on the snowpack structure. Different from what observed for convection in idealized snowpacks, it is further found that (1) sublimation is significant for the whole downward flow not

https://doi.org/10.5194/egusphere-2025-3035
Preprint. Discussion started: 7 July 2025

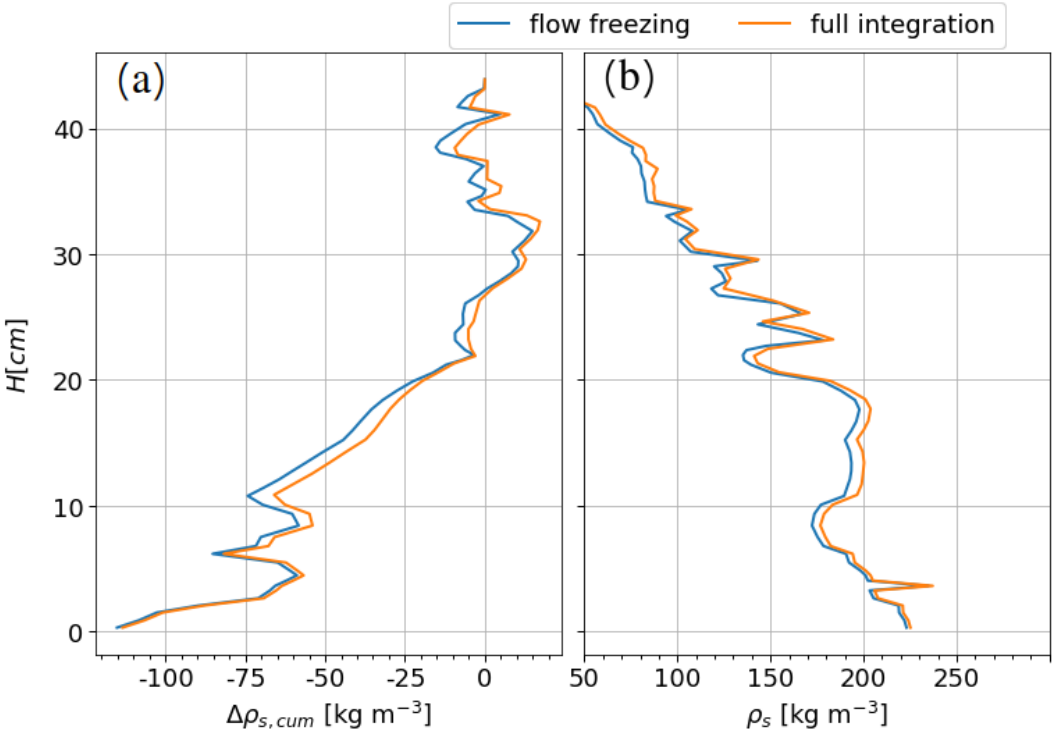

Figure 12. The sensitivity analysis for the difference between "flow freezing" and "full integration" strategies for winter 2017-2018 on 14 April 2018 12:00:00 in Bylot herb tundra, (a) cumulative density change and (b) snow density.

only for the layer close to the ground, (2) the convection cells become more stable over time and do not move laterally, and (3) flow-blocking due to deposition may still move the deposition zone toward the region on top between downward and upward flows. Lateral variations up to 90 kg m^{-3} (115%) for snow density and up to 5 K (30%) for snow temperature indicate major gradients within a convection cell, which may substantially influence secondary processes such as metamorphism and melt-refreeze to laterally vary in the snowpack.

By using SNOWPACK-OpenFOAM coupling, we tested the hypothesis that one-dimensional snow models need to take into account water vapor transport to better capture snow profiles often observed for Arctic snowpacks (i.e. high density on top and lower density in the bottom). The model system simulated in this study leads to a better understanding of the potential impacts of convection in snow covers and how it changes the snow structure, as earlier reported. However, results show a significant difference between observed snow density profiles and simulated ones even when the effects of convection are included (figure 7b, d and f). This shows that the snow model itself needs to be adjusted for Arctic snow covers by further improvements of other important processes shaping the snow profiles such as snow settling and wind compaction. The numerical model used for convection is a direct numerical solution that requires accurate thermo-physical properties, and its comparison with benchmark results shows a numerical accuracy of less than 10% (Jafari et al., 2022). Therefore, to make meaningful

https://doi.org/10.5194/egusphere-2025-3035
Preprint. Discussion started: 7 July 2025

comparisons between simulations and measurements, all snow processes need to be modeled with a similar level of accuracy, which we currently cannot achieve. For Samoylov, as discussed in Jafari et al. (2020), some adjustments for these processes have been already used to have a better representation of snow profiles. Therefore, we need to make the cautionary remark that a realistic high snow density on top - if simulated correctly - could prevent convection, which is a clear limitation of the results discussed above. It needs to be subject of further research, which is not easy as the dynamics of wind compaction are not fully understood and no physics-based model exists, apart from parameterizations as in Gouttevin et al. (2018). As for the Arctic site situated at Samoylov Island, Russia, if we include the effects of wind compaction by using this tailor-made parametrization for new snow density, a layer of high density forms on top. In this case, numerical analysis by SNOWPACK-OpenFOAM coupling shows that if convection occurs, the cells are formed only in the bottom and as a result the net effects of convection are almost negligible. This coupling model only makes sense if tuning and adjustments for these processes (e.g snow settling and wind compaction) do not already include the effects of convection otherwise these effects would be accounted for twice. The lateral variations in snow density within a convection cell, which can reach up to 90 kg m^{-3} (115%), indicate significant gradients within a convection cell in the snowpack. These gradients can substantially influence secondary processes such as metamorphism and melt-refreeze, causing them to vary laterally within the snowpack. As a result, the snow profile can be significantly different depending on where it is measured, i.e., in upward or downward flow. However, making a systematic comparison between simulation and measurement is difficult, if not impossible, due to the complex interplay of different processes affecting the snow structure. This highlights the need for more accurate and comprehensive modeling of all relevant processes, including convection, snow settling, and wind compaction, to better understand the dynamics of snow covers. In this respect, we acknowledge that the results presented in this study may show the upper limit for the effects of convection since (1) the classical grain size is used which induces higher flow velocities than using the optical grain size, (2) the dispersion effects on the thermal and mass transport regimes are not considered which may be important for the bottom of snowpack where the Péclet number is locally greater than 1, and (3) the effects of wind compaction is not considered as discussed above. In any case, future work should address these problems and the current work may serve as a first step into this uncharted land.

Author contributions. MJ started the project by implementing the convective vapor transport in snowpacks by coupling SNOWPACK with OpenFOAM and performed and analyzed the simulations. MJ also prepared the manuscript with the contribution of the second co-author, ML. ML has proposed the main idea behind the project as the supervisor. ML thoroughly revised the paper for submission.

Competing interests. The authors declare that the research was conducted in the absence of any commercial or financial relationships that could be construed as a potential conflict of interest.

https://doi.org/10.5194/egusphere-2025-3035
Preprint. Discussion started: 7 July 2025

Acknowledgements. This project is supported by the Swiss National Science Foundation-SNF, grant number 200021E-154248. Further support by the Swiss National Supercomputing Facility CSCS (grant: S938) is acknowledged.

https://doi.org/10.5194/egusphere-2025-3035
Preprint. Discussion started: 7 July 2025

References

Alley, R., Saltzman, E., Cuffey, K., and Fitzpatrick, J.: Summertime formation of depth hoar in central Greenland, Geophysical Research Letters, 17, 2393–2396, 1990.

Bartelt, P. and Lehning, M.: A physical SNOWPACK model for the Swiss avalanche warning: Part I: numerical model, Cold Regions Science and Technology, 35, 123–145, https://doi.org/10.1016/S0165-232X(02)00074-5, 2002.

Bear, J.: On the tensor form of dispersion in porous media, Journal of Geophysical Research, 66, 1185–1197, 1961.

Bear, J.: Dynamics of fluids in porous media, Courier Corporation, 1988.

Brun, E., Armstrong, R., et al.: Snow and Climate: Physical Processes, Surface Energy Exchange and Modeling, Cambridge University Press, 2009.

Calonne, N., Geindreau, C., Flin, F., Morin, S., Lesaffre, B., Rolland du Roscoat, S., and Charrier, P.: 3-D image-based numerical computations of snow permeability: links to specific surface area, density, and microstructural anisotropy, The Cryosphere, 6, 939–951, https://doi.org/10.5194/tc-6-939-2012, 2012.

Calonne, N., Geindreau, C., and Flin, F.: Macroscopic modeling of heat and water vapor transfer with phase change in dry snow based on an upscaling method: Influence of air convection, Journal of Geophysical Research: Earth Surface, 120, 2476–2497, https://doi.org/https://doi.org/10.1002/2015JF003605, 2015.

Delgado, J.: Longitudinal and transverse dispersion in porous media, Chemical Engineering Research and Design, 85, 1245–1252, 2007.

Derksen, C., Silis, A., Sturm, M., Holmgren, J., Liston, G. E., Huntington, H., and Solie, D.: Northwest Territories and Nunavut snow characteristics from a subarctic traverse: Implications for passive microwave remote sensing, Journal of Hydrometeorology, 10, 448–463, 2009.

Domine, F., Barrere, M., Sarrazin, D., Morin, S., and Arnaud, L.: Automatic monitoring of the effective thermal conductivity of snow in a low-Arctic shrub tundra, The Cryosphere, 9, 1265–1276, 2015.

Domine, F., Barrere, M., and Sarrazin, D.: Seasonal evolution of the effective thermal conductivity of the snow and the soil in high Arctic herb tundra at Bylot Island, Canada, The Cryosphere, 10, 2573, 2016.

Domine, F., BELKE-BREA, M., SARRAZIN, D., ARNAUD, L., BARRERE, M., and POIRIER, M.: Soil moisture, wind speed and depth hoar formation in the Arctic snowpack, Journal of Glaciology, 64, 990–1002, https://doi.org/10.1017/jog.2018.89, 2018.

Domine, F., Lackner, G., Sarrazin, D., Poirier, M., and Belke-Brea, M.: Meteorological, snow and soil data (2013–2019) from a herb tundra permafrost site at Bylot Island, Canadian high Arctic, for driving and testing snow and land surface models, Earth System Science Data, 13, 4331–4348, https://doi.org/10.5194/essd-13-4331-2021, 2021.

Duchesne, D., Gauthier, G., and Berteaux, D.: Habitat selection, reproduction and predation of wintering lemmings in the Arctic, Oecologia, 167, 967–980, https://doi.org/10.1007/s00442-011-2052-0, 2011.

Fahs, M., Graf, T., Tran, T. V., Ataie-Ashtiani, B., Simmons, C., Younes, A., et al.: Study of the effect of thermal dispersion on internal natural convection in porous media using Fourier series, Transport in Porous Media, 131, 537–568, 2020.

Gouttevin, I., Langer, M., Löwe, H., Boike, J., Proksch, M., and Schneebeli, M.: Observation and modelling of snow at a polygonal tundra permafrost site: spatial variability and thermal implications, The Cryosphere, 12, 3693–3717, https://doi.org/10.5194/tc-12-3693-2018, 2018.

Hansen, A. C. and Foslien, W. E.: A macroscale mixture theory analysis of deposition and sublimation rates during heat and mass transfer in dry snow, The Cryosphere, 9, 1857–1878, https://doi.org/10.5194/tc-9-1857-2015, 2015.

https://doi.org/10.5194/egusphere-2025-3035
Preprint. Discussion started: 7 July 2025

Jafari, M.: Water vapor transport in snowpacks, p. 154, https://doi.org/https://doi.org/10.5075/epfl-thesis-9659, 2022.

Jafari, M. and Lehning, M.: snowpackBuoyantPimpleFoam: an OpenFOAM Eulerian–Eulerian two-phase solver for modelling convection of water vapor in snowpacks, https://doi.org/http://dx.doi.org/10.16904/envidat.265, 2021.

Jafari, M. and Lehning, M.: Convection of snow: when and why does it happen?, Frontiers in Earth Science, 11, https://doi.org/10.3389/feart.2023.1167760, 2023.

Jafari, M., Gouttevin, I., Couttet, M., Wever, N., Michel, A., Sharma, V., Rossmann, L., Maass, N., Nicolaus, M., and Lehning, M.: The Impact of Diffusive Water Vapor Transport on Snow Profiles in Deep and Shallow Snow Covers and on Sea Ice, Frontiers in Earth Science, 8, 249, https://doi.org/10.3389/feart.2020.00249, 2020.

Jafari, M., Sharma, V., and Lehning, M.: Convection of water vapour in snowpacks, Journal of Fluid Mechanics, 934, A38, https://doi.org/10.1017/jfm.2021.1146, 2022.

Johnson, J.B., M. S. D. P. and Bens, C.: Field observations of thermal convection in a subarctic snow cover, International Association of Hydrological Sciences Pulblication, 162, 105–118, 1987.

Kvernvold, O. and Tyvand, P. A.: Dispersion effects on thermal convection in porous media, Journal of Fluid Mechanics, 99, 673–686, https://doi.org/10.1017/S0022112080000821, 1980.

Lehning, M., Bartelt, P., Brown, B., Russi, T., Stöckli, U., and Zimmerli, M.: SNOWPACK model calculations for avalanche warning based upon a network of weather and snow stations, Cold Regions Science and Technology, 30, 145–157, https://doi.org/10.1016/S0165-232X(99)00022-1, 1999.

Lehning, M., Bartelt, P., Brown, B., and Fierz, C.: A physical SNOWPACK model for the Swiss avalanche warning Part III: Meteorological forcing, thin layer formation and evaluation, Cold Regions Science and Technology, 35, 169–184, https://doi.org/10.1016/S0165-232X(02)00072-1, 2002a.

Lehning, M., Bartelt, P., Brown, B., Fierz, C., and Satyawali, P.: A physical SNOWPACK model for the Swiss avalanche warning: Part II. Snow microstructure, Cold regions science and technology, 35, 147–167, 2002b.

Moukalled, F., Mangani, L., Darwish, M., et al.: The finite volume method in computational fluid dynamics, vol. 6, Springer, 2016.

Nield, D. and Bejan, A.: Convection in Porous Media, Springer International Publishing, ISBN 9783319495620, https://books.google.ch/books?id=WptcDgAAQBAJ, 2017.

Poirier, M., Fauteux, D., Gauthier, G., Domine, F., and Lamarre, J.-F.: Snow hardness impacts intranivean locomotion of arctic small mammals, Ecosphere, 12, e03 835, https://doi.org/10.1002/ecs2.3835, 2021.

Reid, D. G., Bilodeau, F., Krebs, C. J., Gauthier, G., et al.: Lemming winter habitat choice: a snow-fencing experiment, Behavioral Ecology, 22, 1056–1062, https://doi.org/10.1093/beheco/arr086, 2011.

Sturm, M. and Benson, I. C. S.: Vapor transport, grain growth and depth-hoar development in the subarctic snow, Journal of Glaciology, 43, 42, 1997.

Sturm, M. and Johnson, J. B.: Natural convection in the subarctic snow cover, Journal of Geophysical Research: Solid Earth, 96, 11 657–11 671, https://doi.org/10.1029/91JB00895, 1991.

Taillandier, A.-S., Domine, F., Simpson, W. R., Sturm, M., Douglas, T. A., and Severin, K.: Evolution of the snow area index of the subarctic snowpack in central Alaska over a whole season. Consequences for the air to snow transfer of pollutants, Environmental science & technology, 40, 7521–7527, 2006.

Trabant, D. and Benson, C.: Field experiments on the development of depth hoar, Geological Society of America Memoirs, 135, 309–322, 1972.

https://doi.org/10.5194/egusphere-2025-3035
Preprint. Discussion started: 7 July 2025

Vikhamar-Schuler, D., Hanssen-Bauer, I., Schuler, T. V., Mathiesen, S. D., and Lehning, M.: Use of a multilayer snow model to assess grazing conditions for reindeer, Annals of Glaciology, 54, 214–226, https://doi.org/10.3189/2013AoG62A306, 2013.

Wen, B., Chang, K. W., and Hesse, M. A.: Rayleigh-Darcy convection with hydrodynamic dispersion, Physical Review Fluids, 3, 123 801, 2018.